Spectroscopy of ^{214}Bi and systematics of ^{210,212,214}Pb$(0^+) \xrightarrow{\beta^-} {}^{210,212,214}Bi(0^-)$

Z. Berant*
Brookhaven National Laboratory, Upton, New York 11973,
Clark University, Worcester, Massachusetts 01610,
and Ames Laboratory, Iowa State University, Ames, Iowa 50011

R. B. Schuhmann
Clark University, Worcester, Massachusetts 01610,
and Brookhaven National Laboratory, Upton, New York 11973

D. E. Alburger, W. T. Chou, R. L. Gill, and E. K. Warburton
Brookhaven National Laboratory, Upton, New York 11973

C. Wesselborg
Brookhaven National Laboratory, Upton, New York 11973,
and Justus-Liebig-Universität Giessen, D-6300 Giessen, Germany
(Received 28 December 1990)

Experiments designed to provide more information on the spectroscopy of ^{214}Bi, and on ^{214}Pb$(\beta^-)^{214}$Bi in particular, were undertaken because of interest in first-forbidden β decay in the lead region. The experiments consisted of γ-γ coincidences and angular correlations, conversion electron measurements, level lifetime determinations, and precision γ-ray energy measurements. The 352-keV level of ^{214}Bi was found to be a strong candidate (and the only candidate) for the 0_1^- state. Recent additions to the ^{214}Pb decay scheme are confirmed by γ-γ coincidence measurements. A careful evaluation of the ^{214}Bi level scheme is made with emphasis on separating experimentally based conclusions from speculations based on systematics and other "weak" arguments. Shell-model calculations of the spectroscopy of ^{210,212}Bi and ^{210,212}Pb$(\beta^-)^{210,212}$Bi were performed using a modification of the Kuo-Herling realistic interaction. These calculations and a generalized seniority model provide a basis for an examination of the systematics of the A =210, 212, 214 spectroscopy and β decay. The generalized seniority model is found to be a quite good approximation which provides a quantitative understanding of the ^{214}Pb decay rates.

I. INTRODUCTION

Recent calculations of first-forbidden β^- decay rates of A =205–212 nuclei within the framework of the spherical shell model have achieved an accurate reproduction of experiment.[1,2] First-forbidden decays have contributions from operators which can be classified by rank (R) as rank zero, one, or two. For each decay branch the rate is an incoherent sum of contributions from the ranks allowed by $|J_i - J_f| \leq R \leq J_i + J_f$. Calculations of the fast first-forbidden decays using the impulse approximation achieve agreement with experiment for rank-one ($E1$-like) decays. The rank-two contribution is negligible compared to those of rank zero and one when one or both of the latter are allowed. Agreement with experiment for rank zero is only possible if its total contribution is strongly enhanced over the impulse approximation. Such an enhancement is predicted to arise from meson-exchange currents acting on the matrix element of γ_5 which is the time-like component of the weak rank-zero axial current.[3,4] Thus, the necessary enhancement is parameterized as due to this component alone. The other rank-zero matrix element is the space-like component of the axial current. Proper interpretation of this enhancement is of particular interest and importance since it appears larger than can be explained by calculations of the meson exchange.[1,2] It should be emphasized, however, that no matter how this enhancement is interpreted, the resulting set of effective operators gives a good account of the decays connecting low-lying states in $205 \leq A \leq 212$ nuclei.[1,2]

It is of interest to see how far from A =208 this agreement persists — particularly for the important rank-zero contribution. Accordingly, our attention was focused on ^{214}Pb$(\beta^-)^{214}$Bi for which two very fast decays are reported.[5] A reading of the literature revealed that the

spin assignments in ^{214}Bi, in particular the identification of the 0_1^- level, are uncertain and contradictory.[5,6] We therefore performed γ-γ angular correlations and conversion electron spectroscopy measurements on ^{214}Bi aimed primarily at firmer identification of the 0_1^- level. The angular correlations are the first such measurements reported for this nucleus, while the conversion electron data are in agreement with previous measurements of Mladjenovic and Slätis[7] and Nielsen *et al.*[8] From a combination of all the measurements we deduce firmer spin assignments for the levels in ^{214}Bi, and confirm the 352-keV level as a likely (and only known) candidate for the 0_1^- state.

A recent study proposed two new levels in ^{214}Bi.[9] We performed γ-γ coincidence measurements designed to confirm these results. Information on electromagnetic transition rates provides further valuable tests of the wave functions. We therefore used a β-γ-γ timing method[10] to measure the lifetimes of the 53- and 295-keV levels in ^{214}Bi, in order to provide data on the $M1$ transition rates connecting the low-lying levels of ^{214}Bi. An incidental outcome of these studies is more precise energies for the 53-, 242-, 295-, and 352-keV γ transitions in ^{214}Bi. The experiments are described in the next section and the results are summarized in Sec. III. In Sec. IV we give a simple but seemingly accurate model interpretation of the systematics of first-forbidden β^- transitions leading to ^{210}Bi, ^{212}Bi, and ^{214}Bi.

II. EXPERIMENT

The excited levels in ^{214}Bi were populated via the β^- decay of ^{214}Pb. Figure 1 shows the decay scheme of ^{214}Bi with both our present results and our conclusions regarding previous results incorporated. The results summarized in this figure will be discussed in Sec. III D. The experiment involved five types of measurements: (1) conversion electron spectroscopy, (2) γ-γ angular correlations, (3) β-γ-γ delayed coincidence timing, (4) γ-γ coincidences, and (5) precision γ energies. We describe each in detail in the following sections. All the measurements were performed using sources of 1600 yr ^{226}Ra either in aqueous solution (γ-γ angular correlations) or prepared by drying such a solution (β spectroscopy, γ-γ coincidences, timing, and precision energy). The transitions of interest in ^{214}Bi fall below 800 keV and therefore are well separated from transitions in ^{214}Po which is populated by the β^- decay of ^{214}Bi.

A. Internal conversion measurements

We measured internal conversion electron spectra using a thin radioactive source in conjunction with a Si β detector. The detector was an ORTEC surface-barrier type 1000 μm thick and 100 mm^2 in area. It was chilled to ~ -20°C in order to improve the energy resolution. The source was 10 μCi ^{226}Ra in aqueous solution evaporated

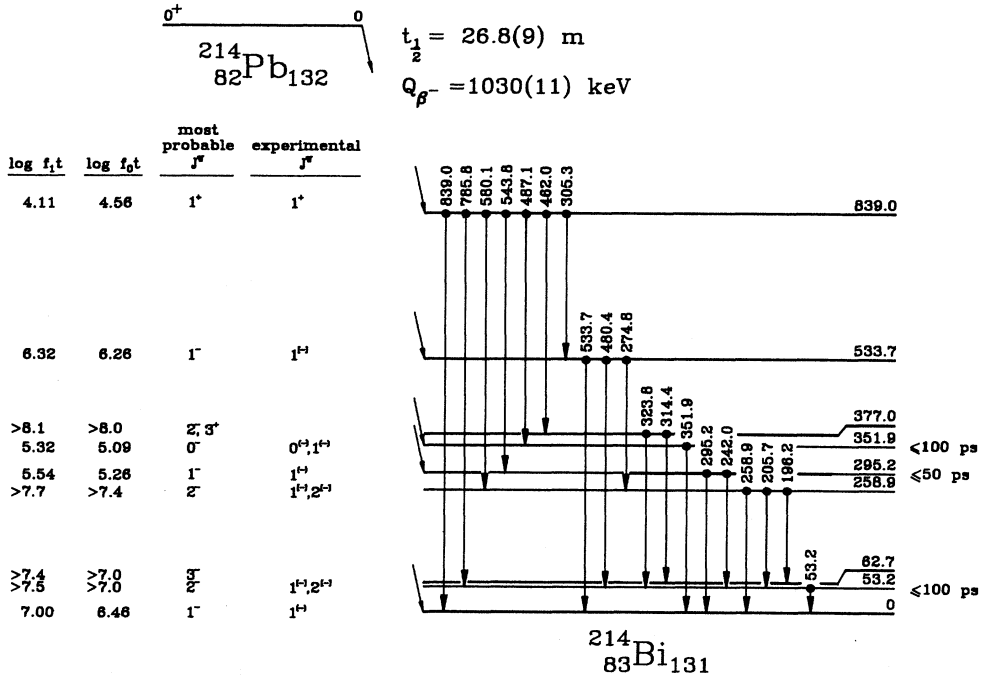

FIG. 1. Decay scheme of ^{214}Bi showing only the γ transitions that have been definitely placed. The spin assignments are derived from a consideration (see Sec. III D) of all experimental information: the present angular correlation and internal conversion measurements, the internal conversion data of Refs. 7 and 8, and $\log f_0 t$ and $\log f_1 t$ values for ^{214}Pb $\rightarrow$ ^{214}Bi and ^{214}Bi $\rightarrow$ ^{214}Po β^- decay. The half-life limits shown are those obtained from the present work for the 53- and 295-keV levels and that of Ref. 11 for the 352-keV level.

onto a 5-mm diameter spot on a plastic disk and covered with a 1-mg/cm^2 thick aluminized Mylar film, the edges of which were sealed with an epoxy resin. The source was mounted in a chamber in He atmosphere 1 cm from the windowless Si detector. Opposite to the β detector and 8.7 cm from the source was a HPGe detector. A thin plastic window in the chamber served to stop β rays but allow low-energy γ rays to pass. The electron and γ spectra were measured simultaneously and are shown in Fig. 2. The upper part of Fig. 2 shows the electron conversion spectrum in the e^- energy range 100–600 keV. The 242-, 295-, and 352-keV transitions take place in ^{214}Bi and the 186-keV line is a transition in ^{222}Rn. The 609-keV transition — the $E2$ $2_1^+ \rightarrow 0_1^+$ decay in ^{214}Po — provided a convenient calibration for internal conversion coefficients (α_j's). In order to obtain absolute α_K and α_L values the relative efficiency of the HPGe detector was determined using a ^{152}Eu source and the γ intensities of the 242-, 295-, 352-, and 609-keV lines (Fig. 2, bottom) were normalized to the relative efficiency. Absolute values of α_K and α_L were deduced via:

$$\alpha_{(K \text{ or } L)} = \frac{I_{(K \text{ or } L)}}{I_\gamma} \frac{0.020\,61 I_{609\gamma}}{I_{609(K+L)}}, \quad (1)$$

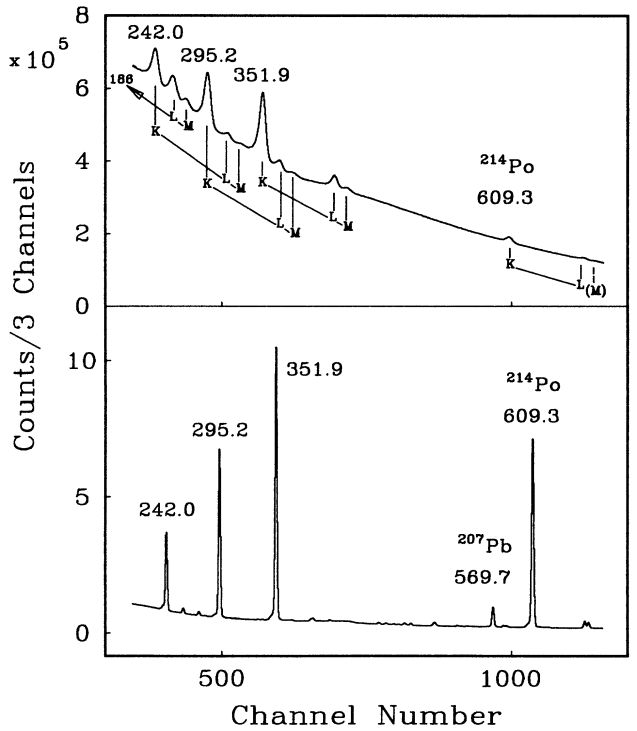

FIG. 2. The upper part of the figure shows the electron conversion singles spectrum for a ^{226}Ra source in the energy range 100–600 keV. The more intense K, L, and M peaks are marked by their associated transition energies. The L and M peaks of a ^{222}Rn line of 186 keV are labeled as such. The lower part of the figure shows the γ-ray singles spectrum in the range 200–700 keV.

where 0.02061 is α_{K+L} for the pure $E2$ 609-keV transition as given in Ref. 22, and $I_{(K \text{ or } L)}$ and I_γ are the corresponding electron and γ peak intensities obtained by using the fitting program LEONE.[12] The α_M were not deduced due to the weak intensity of the M electron conversion peaks and the high background due to the β continuum. The major part of the quoted errors in the conversion coefficients is due to the uncertainties in fitting the areas of the peaks in the presence of this β continuum. As can be seen from Eq. (1), the ratios α_K/α_L are independent of any normalization. We therefore deduced these ratios for the 242-, 295-, and 352-keV transitions from a total of five individual measurements with several different ^{226}Ra sources.

B. Angular correlations

For these measurements we used an aqueous solution containing 10 μCi of ^{226}Ra in equilibrium with its daughters sealed in a glass bottle 1.5 cm diam and 3 cm high. The experimental arrangement was a standard four detector system described in detail elsewhere.[13] The four HPGe detectors (28% efficiency) were placed at a distance of 20 cm from the radioactive source such that angles of 15°, 30°, 45°, 60°, 75°, and 90° were obtained between the various pairs. Data were recorded on-line in event mode and subsequently analyzed off-line. The coincidence energy spectra result from gating the γ spectra with the following photopeak energies: 53, 242, 259, 275, 352, 480, 487, 580, and 786 keV. Examples of coincidence spectra for energy gates set on peaks at 53, 242, 487, and 580 keV are shown in Fig. 3. Integrated peak areas of the coincidences for each angle were normalized by the respective fitted peak areas in the singles spectra. We obtained the coefficients a_2 and a_4 from least-squares fits of the data to the angular correlation function:

$$w(\theta) = a_2 Q_2 P_2(\theta) + a_4 Q_4 P_4(\theta), \quad (2)$$

where the P_k are Legendre polynomials and the Q_k are attenuation coefficients due to the finite solid angles subtended by the γ detectors. In Fig. 4 we present some of the measured angular correlations. The solid lines are the best fits to the Legendre polynomial expansion of Eq. (2). The angular correlation of the 806-609 cascade in ^{214}Po populated via ^{214}Bi decay was obtained simultaneously in the experiment and was used to test the experimental system since this cascade is known to have a spin sequence $0 - 2 - 0$.

C. Half-life measurements

The half-life measurements of the 53- and 295-keV levels were performed using a β-γ-γ fast timing system consisting of BaF_2, plastic, and HPGe detectors. This setup is described in detail in Ref. 10. The radioactive source used in these measurements was the same as used in the conversion electron measurement, with the Mylar β window facing the plastic scintillator. Time spectra were

obtained from β-γ coincidences using pulses from the NE111A plastic detector and the small BaF_2 scintillator as start and stop for an ORTEC-467 time-to-amplitude converter. Triple coincidence with an additional γ line in a HPGe detector selected the decay branch of interest. Previous work[10] with this setup has shown that for β energies greater than 1.5 MeV the timing response of the plastic β detector is independent of β energy. Thus, for $E_\beta > 1.5$ MeV, lifetimes $T_{1/2} > 40$ ps can be obtained from the slope of the delayed coincidence curve, and lifetimes $T_{1/2} > 10$ ps can be determined via the centroid shift of the prompt peak. In the present study, however, the β energy was much lower, 600 keV, and consequently the prompt peaks were non-Gaussian and the timing response is not expected to be independent of β energy. For these reasons, we used only the slope method to study the lifetimes of the 53- and 295-keV levels, since this method is less dependent upon exact knowledge of the prompt peak shape and position. Figure 5 shows the time spectrum obtained by setting the gate in the BaF_2 energy spectrum on the 53-keV γ line and the gate in the HPGe energy spectrum on the 242-keV line. The spectrum shows some tailing on the start side which is due to the low threshold set on the β constant-fraction discriminator to avoid losses in counting rate. We similarly investigated the lifetime of the 295-keV level by setting the BaF_2 gate on the 242-keV γ line and the gate in the HPGe spectrum on the 53-keV line. We obtained a prompt time spectrum using a ^{60}Co source with a thin β window and scanning with the energy gate for the BaF_2 detector on the Compton region at the same position as for the 53- or 242-keV gates. The HPGe energy gates were set on both the 1173- and 1333-keV peaks.

D. γ-γ coincidences

In a recent γ-γ coincidence study of ^{214}Pb(β^-)^{214}Bi γ rays, Mouze *et al.*[9] proposed new ^{214}Bi levels at 62.68 and 377.07 keV. These two levels, shown in Fig. 1, would appear to explain the previously unplaced (but assigned to ^{214}Pb) γ rays[5] of 196.3(5), 314.2(4), 324.3(5), and 462.1(2) keV. There is no strong information as to the

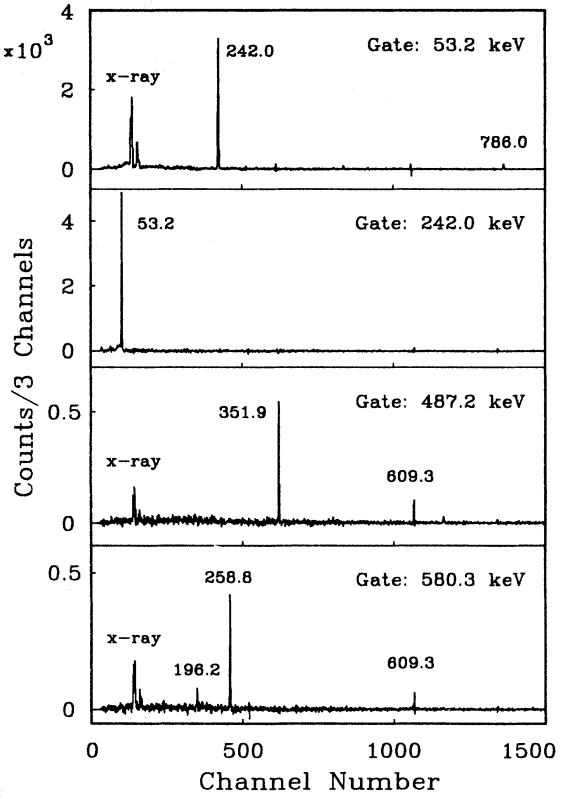

FIG. 3. Examples of coincidence spectra obtained in the angular correlation measurements obtained with energy gates on the peaks of 53, 242, 487, and 580 keV. Gamma-ray energies are in keV. The placement of the transitions is given in Fig. 1.

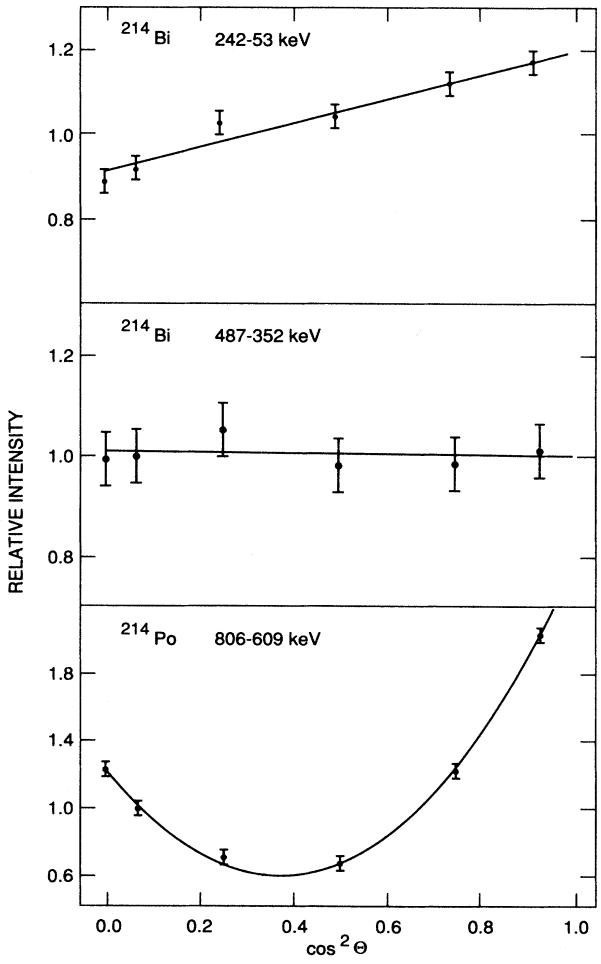

FIG. 4. The two upper figures are the angular correlations for the 242-53 and 487-352 cascades in ^{214}Bi. The lower figure is the angular correlation for the $0-2-0$ 806-609 cascade in ^{214}Po. The solid lines are the best fits to $w(\theta) = a_2 Q_2 P_2(\theta) + a_4 Q_4 P_4(\theta)$, i.e., to Eq. (2).

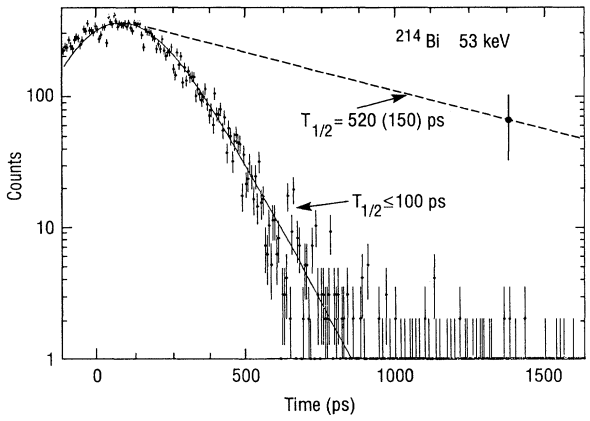

FIG. 5. Time spectrum for the decay of the ^{214}Bi 53-keV level. The solid curve is a least-squares fit to the data assuming an exponential decay superimposed on a Gaussian peak. The fit to the prompt ^{60}Co time spectrum (see text) is indistinguishable to the eye from the fit shown which corresponds to an exponential slope with $T_{1/2} = 72$ ps. The dashed exponential decay indicates a 520-ps half-life with an error bar of ±150 ps as reported in Ref. 11.

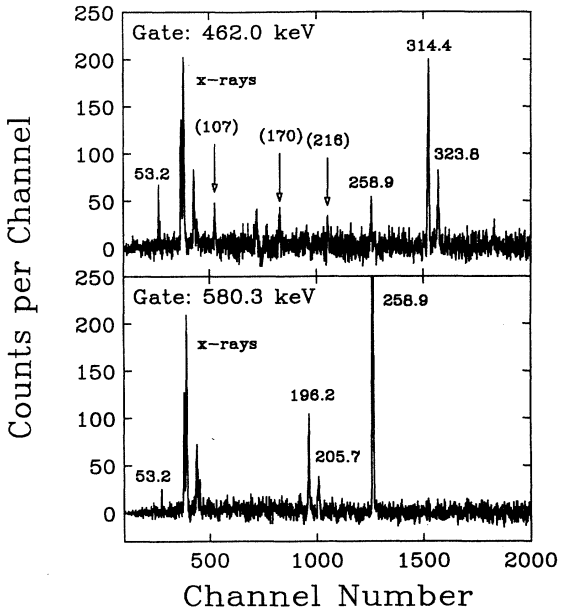

FIG. 6. Coincidence spectra obtained with energy gates on the peaks of 462 and 580 keV. Gamma-ray energies are in keV. The peaks whose energies are enclosed in parentheses are not considered as definitely established. The remaining transitions are placed in the level scheme of Fig. 1. The "peak" between those labeled (107) and (170) in the 462-keV gate spectrum is due to backscattering of the intense ^{214}Po 609-keV transition from one detector to the other.

J^{π} values of these two levels.

We performed γ-γ coincidence measurements in a close geometry using two HPGe and one LEPS (low-energy-photon-spectrometer) detector and were able to confirm the following coincidence relationships: (1) the 314- and 324-keV γ rays with the 462-keV transition, and (2) the 196-keV γ ray with both the 580- and 275-keV transitions. Partial spectra in coincidence with gates on the 462- and 580-keV transitions are shown in Fig. 6. These results are not as complete as those of Mouze *et al.*[9] but independently support the proposed existence of the 63- and 377-keV levels. Note that other placements of the γ transitions in question are possible. However, any other placement demands at least one more level and an unlikely equality of unassociated γ-ray energies or their sums.

Mouze *et al.*[9] also observed γ transitions of 107.2, 170.0, and 216.4 keV in coincidence with the 462-keV transition but did not consider these transitions to be definitely assigned to ^{214}Bi. As shown in Fig. 6 we also observe suggestive evidence for these three transitions in the spectrum in coincidence with the 462-keV gate. We also hesitate to make a definite assignment of these transitions to ^{214}Bi. Further work is necessary to establish the placement of these lines.

TABLE I. Results of precision γ-ray energy measurements on ^{210}Pb(β^-) and ^{214}Pb(β^-). For each reference source at least two γ-ray peaks were utilized; only the principal one is listed.

Nucleus	Reference γ ray E_γ (keV)	Ref.	No. of measures	Pb(β^-) E_γ (keV) Measured	Adopted	Previous
^{241}Am	59.5364(10)	a	10	46.5385(21)[b]	46.5385(21)[b]	46.520(20)[b]
^{241}Am	59.5364(10)	a	10	53.2230(21)	53.2230(21)	53.226(14)[c]
^{152}Eu	244.6989(10)	d	21	241.9983(30)	241.998(3)	241.987(8)
^{133}Ba	302.853(1)	e	12	295.226(2)	295.226(2)	295.220(8)
^{152}Eu	344.2811(19)	d	21	351.9300(24)	351.932(2)	351.930(8)
^{133}Ba	356.017(2)	e	12	351.9339(24)		

[a]Reference 18.
[b]^{210}Pb(β^-).
[c]Reference 19.
[d]Reference 16.
[e]Reference 21.

E. Precision energy measurements

In an earlier experiment[14,15] the γ-ray energies of the 295 $\rightarrow$ 53, 295 $\rightarrow$ 0, and 352 $\rightarrow$ 0 transitions were determined as 241.987(8), 295.220(8), and 351.930(8) keV, respectively. Using a well-established mixed-source technique with procedures designed to minimize systematic uncertainties[16,17] we reduced the uncertainties to 3 eV or less for these transitions and the 53 $\rightarrow$ 0 transition as well. The remaining uncertainty is largely due to the precision with which energies can be extrapolated in the vicinity of the calibration energies and to the uncertainties in the calibration lines themselves. Following the methodology outlined previously[17] we simultaneously measured the γ spectra due to the decay of ^{214}Pb and standard reference sources, using a LEPS detector. Numerous sets of runs were made, in each of which a variety of amplifier gain settings, analyzer digital offsets, and source-to-detector distances were used. Care was taken to avoid systematic errors due to random summing and to the presence of weak unresolved γ-ray lines. Examples are the presence of a 243.56-keV peak in the ^{152}Eu spectrum due to random summing of two 121.78-keV peaks, and the proximity of the ^{152}Eu 295.96-keV γ peak to the 295.23-keV peak of ^{214}Pb. In the analysis of the data the peak positions were obtained using the program LEONE,[12] which fits a Gaussian peak shape on a background consisting of a step function under the peak superposed on a polynomial function.

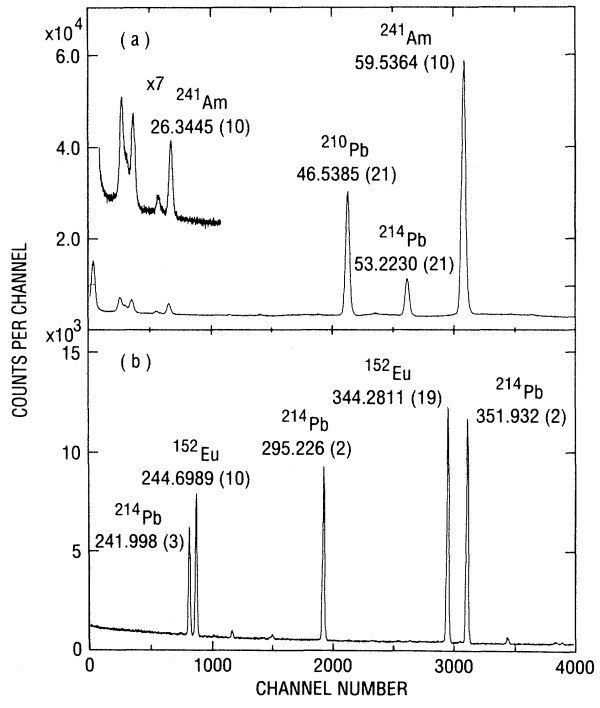

FIG. 7. Two of the runs for ^{214}Bi precision E_γ determinations using the mixed-source technique and a LEPS detector. Energies are in keV and the adopted values are shown for the ^{214}Pb(β^-)^{214}Bi γ rays.

Table I summarizes the results of the precision γ-ray energy measurements and Fig. 7 illustrates typical spectra. The next to last column of Table I gives the adopted values for the ^{214}Pb(β^-) γ rays. All are in agreement with the previous results shown in the last column, but the uncertainties have been reduced substantially. We note that the sum 53.223(2) + 241.998(3) = 295.221(4) keV agrees within the uncertainties with the direct measurement of 295.226(2) keV for the ground-state transition. Thus the weighted-average value for the excitation energy is 295.225(2) keV.

III. EXPERIMENTAL RESULTS

A. Internal conversion coefficients

The results of the internal conversion coefficient measurements are summarized in Table II. The accuracy of our data regarding the ratios α_K/α_L is comparable to previous measurements.[7,8] In order to obtain information on the multipolarities of the 53-, 242-, 295-, and 352-keV transitions, a least-squares fit was made for each transition to the K, L, M $(N+O)$ data from Ref. 7, the present K/L ratios (Table II) and the K/L data of Ref. 8 (also included in Table II). The function fitted was

$$R_{ij} = \frac{\alpha_i(M1)_{\rm th} + \delta^2\alpha_i(E2)_{\rm th}}{\sum_j \left[\alpha_j(M1)_{\rm th} + \delta^2\alpha_j(E2)_{\rm th}\right]}. \quad (3)$$

In Eq. (3) R_{ij} is the measured ratio between the normalized peak intensities of conversion electrons of shell i to a sum over those for a set of shells j; the sum is over the L shell for the K/L ratios and over all measured shells for the data of Mladjenovic and Slätis;[7] $\alpha_j(M1)_{\rm th}$ and $\alpha_j(E2)_{\rm th}$ are the theoretical α_j values for $M1$ and $E2$ radiation,[22] respectively, and δ is the $E2/M1$ mixing ratio. Our results are in satisfactory agreement with previous results. They are close to the theoretical predictions for $M1$ radiation and indicate that the major component in the 242-, 295-, and 352-keV transitions is $M1$. However, our conclusions for the restrictions on the $E2/M1$ mixing ratio, δ, are considerably less restrictive than those given in the last two compilations.[6,5] The results given in the last two columns of Table II were arrived at after a careful appraisal of the consistency of the various spectroscopic data. The main problem which demands this care is that the data of Mladjenovic and Slätis[7] — although of high-energy dispersion and thus valuable — were taken with photographic emulsions thereby giving the relative intensities large errors which are difficult to assess. We demanded that their data be internally consistent with a chi squared per degree of freedom, χ^2_D, of unity or less before combining them with the α_K/α_L ratios of Table II. We also examined the effect of varying the relative uncertainties. We conclude that the more restrictive values of δ cited in the compilations result from unjustifiably low uncertainties on the relative intensities and concomitant unacceptably high values of χ^2_D.

TABLE II. Internal conversion results for electromagnetic transitions in ^{214}Pb $\rightarrow$ ^{214}Bi β^- decay. The present experimental results for α_K and α_L are given in the third column while present and previous α_K/α_L values are given in the sixth column. The theoretical (th) values for α_K and α_L are from Ref. 22. The limits for δ^2 — where δ is the $E2/M1$ mixing ratio — were derived from a least-squares fit to the listed results and the previous K, L, M $(N+O)$ data of Ref. 7.

Shell (j)	E_γ (keV)	α_j	$\alpha_j(M1)_{th}$	$\alpha_j(E2)_{th}$	α_K/α_L	δ^2	$\lvert\delta\rvert$
L	53		9.606	96.82		<0.0030[a]	<0.055[a]
M	53		2.255	25.49			
K	242	0.73(16)	0.7126	0.1099	6.97(51)	<0.24[b]	<0.50[b]
L	242	0.104(26)	0.1235	0.0963	5.30(15)[c]		
K	295	0.418(38)	0.4123	0.0692	5.29(23)	<0.24[b]	<0.50[b]
L	295	0.082(10)	0.0714	0.0440	5.55(15)[c]		
K	352	0.280(23)	0.2555	0.0463	5.81(15)	<0.077[b]	<0.28[b]
L	352	0.049(5)	0.0442	0.0229	5.65(15)[c]		

[a]One standard deviation.
[b]Two standard deviation.
[c]Reference 8.
[d]Reference 7 and Sec. III D.

B. Angular correlations

Table III summarizes the results of the γ-γ angular correlations measurements. The values of a_2 and a_4 reported in Table III are corrected for the geometrical factors Q_2 and Q_4 [see Eq. (2)]. As can be seen from Table III the a_4 values for all the cascades measured for ^{214}Bi are consistent with zero within the error limits as expected if one or both of the two members of the cascade has a small or vanishing quadrupole component. The angular correlations of the first five listed cascades have a_2 values close to those expected for a pure dipole $1-2-1$ cascade for which $a_2 = +0.175$ is expected. The 839 $\rightarrow$ 352 $\rightarrow$ 0 cascade is isotropic within errors, and the ^{214}Po 1415 $\rightarrow$ 609 $\rightarrow$ 0 cascade has a_k values consistent with the expected values for a $0-2-0$ cascade of $a_2 = +0.357$, $a_4 = +1.143$.

Analysis of the angular distribution data (e.g., Fig. 4) proceeded as follows: a spin sequence $J_1 - J_2 - J_3$ was assumed, such as $1-1-1$, and the mixing ratio for one of the two transitions was fixed at a particular value. Then least-squares fits were made to $w(\theta)$ for selected values of the mixing ratio, δ, of the other transition. We use the sign convention of Biedenharn and Rose[23] for the mixing ratios. Actually, $\tan^{-1}\delta$ was varied between $-90°$ and $+90°$ in appropriate steps and plots were constructed of χ^2_D vs $\tan^{-1}\delta$. Quantitative analysis of the results to choose allowable spin sequences and mixing ratios relies heavily on proper error analysis. Thus a first step in the analysis was to assume a constant systematic uncertainty Δ_s applicable to each datum, to form the uncertainty for a particular point as the sum in quadrature of the statistical and systematic uncertainties, and to choose Δ_s such that the total ensemble of all seven angular distribution fits of Table III had a χ^2_D of unity. The result was $\Delta_s = \sim 1.5\%$.

TABLE III. Gamma-gamma angular correlation results following the β^- decay of ^{214}Pb to ^{214}Bi. The 806-609 $0-2-0$ cascade in ^{214}Po is also included. The limits (one standard deviation) on the mixing ratio δ refer to the upper member of the cascade and were derived using the limits of Table II for the mixing ratio of the lower member of the cascade.

Cascade (keV)	Initial level (keV)	a_2	a_4	Spin sequence	δ lower	δ upper
242 – 53	295	+0.194(24)	−0.027(31)	1 – 1 – 1	−0.28	+0.00
				1 – 2 – 1	−0.07	+0.14
480 – 53	534	+0.156(62)	+0.028(85)	1 – 1 – 1	−0.33	+0.11
				1 – 2 – 1	−0.17	+0.19
786 – 53	839	+0.207(77)		1 – 1 – 1	−0.45	−0.02
				1 – 2 – 1	−0.05	+0.30
275 – 259	534	+0.131(63)	−0.040(86)	1 – 1 – 1	no useful limit	
				1 – 2 – 1	no useful limit	
580 – 259	839	+0.156(39)	−0.056(56)	1 – 1 – 1	no useful limit	
				1 – 2 – 1	no useful limit	
487 – 352	839	−0.011(29)	−0.006(40)	1 – 0 – 1	0.00	0.00
				1 – 1 – 1	−0.09	+0.40
806 – 609	1415	+0.343(21)	+1.087(37)	0 – 2 – 0	0.00	0.00

Examples of the χ^2_D vs $\tan^{-1}\delta$ plots are shown in Figs. 8 and 9. Because of the similarity in the angular distributions, plots for the first five cascades of Table III are similar and can be discussed with reference to Figs. 8 and 9. In the analysis of these data we assume that the ^{214}Bi ground state has $J = 1$ (see Sec. III D 1) and consider spins of J=0,1,2 for the other levels of Table III. The anisotropy of the angular correlations rules out J=0 for the 53- and 259-keV levels. We show the results for an assumption of $J = 0$ for the 295-keV level in Figs. 8 and 9. Within the allowable values for the $53 \rightarrow 0$ mixing ratio (see Table II), the solution for this assumption is well above the 0.1% probability limit and is thereby rejected. A similar result is obtained for the first five cascades of Table III. Thus we can reject the J=0 possibility for the levels at 53, 259, 295, 534, and 839 keV but not for that at 352 keV. This is the bulk of the information obtainable from the angular correlations. There are also some restrictions on mixing ratios which are indicated in Table III. As can be surmised from Figs. 8 and 9, we can rule out a J=2 assignment for the 295-keV level; however, as discussed in Sec. III D below, a $J = 2$ assignment is also ruled out by the $\log f_1 t$ value for the ^{214}Pb decay to this level.

Previous evidence[5] excludes the $J = 3$ possibility for

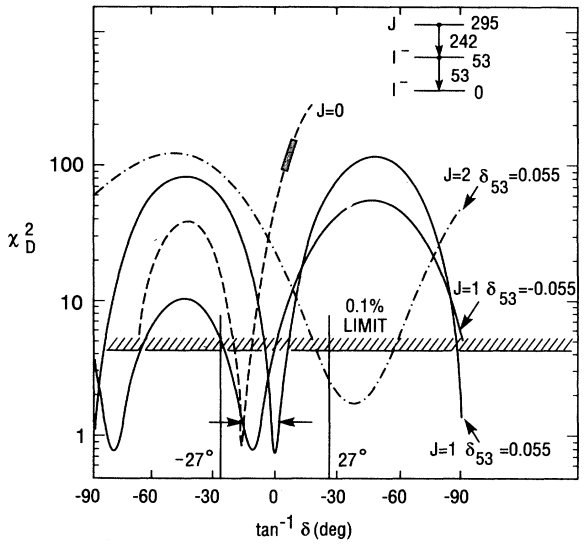

FIG. 8. χ^2_D vs $\tan^{-1}\delta$ plots for the 242–53 cascade assuming the spin sequence $J - 1 - 1$. δ is the quadrupole-to-dipole mixing ratio for the 242-keV transition. The dashed curve is for $J = 0$ (with δ_{53} varied rather than δ_{242}) and the rectangle marked on the curve shows the allowed region for $|\delta_{53}| < 0.055$ — where this limit on δ_{53} is from Table II. The two solid curves are the $1 - 1 - 1$ results for $\delta = +0.055$ and -0.055, respectively. The dash-dotted curve represents the $2 - 1 - 1$ spin sequence for $\delta_{53} = +0.055$. Vertical lines at $\tan^{-1}\delta = \pm 27°$ delineate the region allowed for δ_{242} by the internal conversion results of Table II. The one standard deviation limits, $-0.28 \leq \delta_{242} \leq +0.04$, for the $1 - 1 - 1$ assumption are indicated by the horizontal arrows.

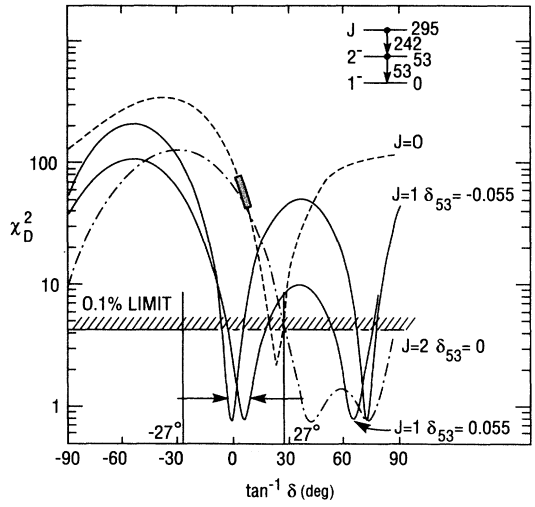

FIG. 9. χ^2_D vs $\tan^{-1}\delta$ plots for the 242–53 cascade assuming the spin sequence $J - 2 - 1$. The dashed curve is for $J = 0$ (with δ_{53} varied rather than δ_{242}) and the rectangle marked on the curve shows the allowed region for $|\delta_{53}| < 0.055$ — where this limit on δ_{53} is from Table II. The two solid curves are the $1 - 2 - 1$ results for $\delta_{53} = +0.055$ and -0.055, respectively. The dash-dotted curve represents the $2 - 2 - 1$ spin sequence for $\delta = 0$. Vertical lines at $\tan^{-1}\delta = \pm 27°$ delineate the region allowed for δ_{242} by the internal conversion results of Table II. The one standard deviation limits, $-0.07 \leq \delta_{242} \leq +0.14$, for the $1 - 2 - 1$ assumption are indicated by the horizontal arrows.

all levels of Fig. 1 except the 259-keV level. A fit of the $839 \rightarrow 259 \rightarrow 0$ angular correlation to the spin sequence $1 - 3 - 1$ yielded no solution for any combination of the two mixing ratios below the 1% confidence level. This is ample grounds to reject the $J = 3$ possibility for the 259-keV level. Furthermore, because of the symmetry of this decay sequence the two mixing ratios are interchangeable. For one mixing ratio constrained by $|\delta| < 0.3$ and the other mixing ratio unconstrained, all solutions are above the 0.1% confidence limit. If the ground state and 839-keV level have different parities — as is highly likely (see Sec. III D) — one of the two transitions would necessarily be an $M3/E2$ mixture, a $|\delta| > 0.3$ for it would be quite unlikely. We conclude that the 259-keV level has $J = 1$ or 2. Finally, with the assumption that the γ decays from the 839-keV level are mixed $E1$ and $M2$ it is likely that the $M2$ component is negligible. If so, the $839 \rightarrow 259 \rightarrow 0$ angular correlation yields $\delta_{259} = +0.03(6)$ or $+0.12(3)$ depending on whether the 259-keV level is $J = 2$ or 1.

C. Half-life measurements

Figure 5 shows the time spectra for the 53-keV transition which should reflect the half-life of the 53-keV level. A comparison with the corresponding prompt spectra ob-

tained from ^{60}Co indicates no discernible delay for the ^{214}Bi transitions. From the slope of the tails of the time spectra we deduce an upper limit for the half-lives of both the 53- and 295-keV levels. The ^{60}Co and ^{214}Pb time spectra were fitted with a function containing a Gaussian distribution and an exponential tail. For the 53-keV window on the BaF_2 detector — giving the sum $T_{1/2}(295)+T_{1/2}(53)$ — the results of the fits for both the ^{214}Pb and ^{60}Co β-γ timing show a full width at half maximum (FWHM) of the time peaks of 260 ps and indistinguishable slopes on the stop side (see Fig. 5). From this we conclude that the combined half-lives of the 295- and 53-keV levels is <100 ps and, therefore, $T_{1/2}(53\text{ keV}) <$ 100 ps represents a conservative upper limit. This result disagrees with the value of 520(150) ps obtained by Penev *et al.*[11] using the centroid shift method. We emphasize that with the present time resolution (FWHM=260 ps) for the 53-keV γ ray a 520-ps half-life could easily be observed in the time delay spectrum (as indicated by the dashed line in Fig. 5). The time spectrum of the 242-keV γ line is narrower (FWHM=180 ps) due to the higher γ energy. Following a similar procedure of fitting the time spectra an upper limit $T_{1/2}(295\text{ keV}) < 50$ ps was obtained. This value lowers the upper limit for the half-life of the 295-keV level [$T_{1/2}(295\text{ keV}) \leq 100$ ps] as given by Penev *et al.*[11] by a factor of 2.

D. Synthesis of results and ^{214}Bi spin-parity assignments

In this section we will first analyze the experimental spectroscopic information on ^{214}Bi and arrive at our appraisal of the rigorously proven (labeled "experimental") spin-parity values for the ^{214}Bi levels of Fig. 1. We will then invoke other (weaker) arguments to arrive at the most probable spin-parity values shown in Fig. 1. β and γ branching ratios and transition and level energies were calculated from the γ-ray energies and intensities of Mouze *et al.*[9] and the present results. The β^- branching ratios, decay rates, and $\log f_0 t$ (allowed) values are listed in Table IV together with the adopted level energies. The results of Table IV and Fig. 1 were obtained from the primary data using the least-squares-fitting program GTOL of the National Nuclear Data Center.[24–26]

TABLE IV. Summary of ^{214}Bi level energies and ^{214}Pb(β^-)^{214}Bi branching ratios and $\log f_0 t$ values. The numbers in parentheses are the uncertainties in the last figure.

^{214}Bi level (keV)	β^- branching ratio (%)	$\log f_0 t$
0.0	8.5(10)	6.459(56)
53.224(2)	<1.7	>7.0
62.68(5)	<1.7	>7.0
258.87(2)	<0.34	>7.4
295.225(2)	41.09(24)	5.263(27)
351.932(2)	46.7(7)	5.088(29)
377.03(4)	<0.05	>8.0
533.671(14)	1.11(7)	6.257(53)
838.99(2)	2.58(11)	4.561(82)

1. Consideration of log $f_0 t$ and log $f_1 t$ values

A recommended strong rule for spin-parity assignments via beta decay is *first-forbidden unique β transitions have* $\log f_1 t \geq 8.5$.[27] As seen in Fig. 1, none of the indicated ^{214}Pb → ^{214}Bi decays so qualify and we assign $J < 2$ to the levels at 0, 295, 534, and 839 keV. After combining with our angular correlation result of $J \neq 0$, we have $J = 1$ assignments to the levels at 295, 534, and 839 keV. The rule given above for first-forbidden unique transitions and a similar one for second-forbidden transitions[27] can be used to yield $J \neq 0$ for the ^{214}Bi ground state since it decays to several ^{214}Po 2^+ states with $\log f_1 t < 8.5$.[28]

The ^{214}Pb → ^{214}Bi $\log f_0 t$ value of 4.6 (Fig. 1) has been used to assign $J^\pi = 1^+$ to the 839-keV level. Our independent exclusion of $J = 0$ strengthens this argument since, from local systematics, the next most likely assignment would appear to have been $J^\pi = 0^-$. There are no known parity-changing $\Delta J = 1$ β transitions with $\log f_0 t < 5.2$ and so we also adopt $J^\pi = 1^+$ for the 839-keV level.

2. The parity of the ^{214}Bi levels at 0, 53, 295, and 352 keV

In Sec. II A we described our procedure for setting upper limits on the $E2$ component in the 53-, 242-, 295-, and 352-keV transitions from internal conversion information. Since the α_j for $E1$ and $M2$ radiation fall below and above, respectively, the values possible for $E2/M1$ radiation, it is usually possible to find an $M2/E1$ ratio for which the experimental data are reproduced as well (or nearly) as for $E2/M1$ radiation. Thus least-squares fits were also made to experiment with the $M2$ and $E1$ theoretical α_j substituted for the $E2$ and $M1$ values in Eq. (1). It was found that the internal conversion data for the 53-keV transition could only be fitted assuming $E2/M1$ radiation but that the 242-, 295-, and 352-keV transitions had acceptable solutions for $M2/E1$ δ^2 values of 0.38(7), 0.31(1), and 0.35(1). The quite restrictive uncertainties on the $M2/E1$ ratios are a result of the very different α_j values for $M2$ and $E1$ radiation, e.g., $[\alpha_K(E1)_{\text{th}}, \alpha_K(M2)_{\text{th}}] = [0.04132, 2.6890]$ for the 242-keV transition. If now we combine these $M2/E1$ ratios with the lower limits on the level lifetimes (see Fig. 1) and the transition branching ratios, we find the $M2$ transition strengths are well above any reasonable limit; e.g., the $M2$ strength of the 352-keV transition is greater than 320 single-particle (Weisskopf) units. We conclude that the ^{214}Bi levels at 0, 53, 295, and 352 keV can definitely be assigned the same parity.

We next ask what information we have as to the parity of these four levels. ^{214}Pb → ^{214}Bi → ^{214}Po $\log f_0 t$

TABLE V. Internal conversion results for weaker electromagnetic transitions in ^{214}Pb → ^{214}Bi β^- decay. The theoretical (th) values for α_K and α_{L1} are from Ref. 22. The estimates of the experimental α_j utilize the data of Ref. 7 as explained in the text (Sec. III D).

Shell (j)	E_γ (keV)	α_j	$\alpha_j(M1)_{th}$	$\alpha_j(E2)_{th}$	$\alpha_j(E1)_{th}$	$\alpha_j(M2)_{th}$	$\lvert\delta\rvert$
K	259	~0.58	0.5924	0.0941	0.0352	2.1510	$\lesssim 1.00$
$L1$	259	~0.10	0.0922	0.0137	0.0044	0.4618	
K	275	~0.52	0.5021	0.0818	0.0306	1.7660	$\lesssim 1.00$
$L1$	275	~0.08	0.0782	0.0119	0.0038	0.3734	
K	487	<0.024	0.1077	0.0228	0.0086	0.2955	
K	580	<0.024	0.0677	0.0159	0.0061	0.1763	
K	786	<0.009	0.0308	0.0088	0.0034	0.0745	

values are no help because all relevant decays could be allowed or first-forbidden nonunique. The only source of useful information is internal conversion measurements on transitions connecting the ^{214}Bi 1^+ 839-keV level to the lower-lying states. The α_K values of the 487-keV 839 → 352 and 786-keV 839 → 53 transitions are given in Table V. This information comes from the magnetic spectrometer results of Mladjenovic and Slätis,[7] which had sufficient energy resolution to resolve these lines from others. They did not report the observation of any decays from the 839-keV level. Following Lingeman *et al.*[25] we assume the intensity of these lines is less than that of the weakest line they observed in the nearby energy regions (e^- energies of 765 and 392 keV), and derive limits on the possible α_K from the normalization of Eq. (1). However, these limits were increased by 30% to allow for the uncertainties in the normalization. Theoretical α_K values are given in Table V for $M1$, $E2$, $E1$, and $M2$ radiation. If the transitions are assumed to be predominantly dipole then $E1$ radiation is strongly favored; thus, if the 352 keV has $J = 0$ the case for odd parity is strong. However, in the absence of proof of this $J = 0$ assignment, strongly mixed $E2/M1$ radiation is certainly possible for all three transitions. We conclude that this information strongly favors odd parity for the low-lying states in question but is not conclusive. This conclusion is less restrictive than previous studies, e.g., Ref. 25, and compilations[5] which gave the ground state of ^{214}Bi a definite $J^\pi = 1^-$ assignment. However, it appears that shell-model arguments were invoked in the compilation[5] whereas we have chosen to present assignments based solely on strong experimental arguments.

3. The 259- and 534-keV levels

We next consider the parities of the 259- and 534-keV levels. Once again, the available information is the internal conversion measurements of Mladjenovic and Slätis[7] which is summarized in Table V. The relevant decays are the 275-keV 534 → 259 and 259-keV 259 → 0 transitions and the 580-keV 839 → 259 transition. For the first two of these decays the α_j information, derived using Eq. (1), is in good agreement with $M1$ radiation and readily excludes pure $E1$ radiation. Both could be mixed $M2/E1$ decays and from them we only give most probable odd-parity assignments to the 259- and 534-keV levels. Like the other two decays from the 839-keV level the 839 → 259 transition was not observed and we arrive at a limit as explained above. For this transition $E1$ radiation is favored for the same reasons and to the same extent as for the 839 → 352 and 839 → 53 transitions. This gives further support to an odd-parity assignment to the 259-keV level.

4. The 63- and 377-keV levels

A noticeable feature of the γ decays involving the 63- and 377-keV levels (see Fig. 1) assigned by Mouze *et al.*[9] and confirmed by us (Sec. II D) is the nonobservation of γ decays from the 62.68-keV level. To provide more information on these decays, we examined singles spectra such as that in the upper panel of Fig. 7 (but with considerably higher statistics and no ^{241}Am), and set the two-standard-deviation limit $I_\gamma(63)/I_\gamma(53) < 0.003$. This absence of a 63 → 0 γ transition turns out to be not surprising at all. We note that a 9.47-keV 63 → 53 transition would not have been observed in previous studies. Assuming odd parity for the 63-keV level, the two most likely spin assignments are $J = 2$ or 3. If $J^\pi = 2^-$, both possible γ decay modes would be expected to be $M1$. Taking the feeding intensity for the 63-keV level, $I(196)+I(314)$, from the γ-ray intensities of Mouze *et al.*[9] and the assumption of pure $M1$ transitions, we find an upper limit on the branching ratio of the 63-keV ground-state transition of <9%. If, on the other hand, the 63-keV level were $J^\pi = 3^-$ so that the 63 → 0 transition were $E2$ and the 63 → 53 transition were $M1$, the γ decay of the 63-keV level would be overwhelmingly ($\approx$ 99.9%) to the 53-keV level.[29] Thus, in either case it is expected that the 63 → 53 transition is the dominant decay mode.

5. Summary of spin-parity assignments and β^- decay rates

To summarize, our conclusions for the rigorously proven spin-parity values for ^{214}Bi are in the column labeled "experimental" in Fig. 1. The levels for which the

parity is enclosed in parentheses all have the same parity and with a high probability that parity is odd while the parities enclosed in square brackets are more probably odd than even.

If we invoke the shell model — or even local systematics — the case for odd parity for the nine low-lying states of Fig. 1 is very strong indeed and this is so indicated in the "most probable" column of Fig. 1. The choice of spin assignments follows from the $\log f_0 t$ value for the 352-keV level, the absence of observable β^- decays to the 53-, 63-, 259-, and 377-keV levels, the γ decay modes, and the shell-model expectations which will be presented in Sec. IV. In the remainder of this article we shall assume the most probable J^π values of Fig. 1.

IV. MODEL PREDICTIONS OF β^- AND γ DECAY RATES

A. Shell-model calculations for A =210 and 212

Shell-model calculations for ^{210}Bi and ^{212}Bi and for ^{210}Pb$(\beta^-)^{210}$Bi and ^{212}Pb$(\beta^-)^{212}$Bi were performed using the KHP$_e$ interaction[30] which operates in the particle space above ^{208}Pb shown in Fig. 10. Calculations for $A = 214$ in the KHP model space are beyond our computational resources. Thus, as will be discussed, we resort to a simplifying approximation in order to attempt an understanding of the nuclear structure of ^{214}Pb and ^{214}Bi. But first we describe calculations carried out for $A = 210$ and 212 with the spherical shell-model code OXBASH.[31] The results of these calculations will provide the basis for an extrapolation to $A = 214$. The KHP$_e$ interaction uses as its basis the Kuo-Herling interaction[32] but with modifications to better reproduce the binding energies and energy spectra of $A = 210 - 212$ nuclei.[30] In particular, relevant neutron-proton two-body matrix elements (TBME) were varied so as to reproduce — essentially exactly — the low-lying ($E_x < 2.0$ MeV) spectrum of ^{210}Bi. The energy spectrum of ^{212}Bi was calculated with this interaction.[33] A comparison is made to the experimentally known low-lying spectrum in Fig. 11. The J dimensions of the KHP$_e$ spectrum peak at 4509 for $J = 5$. The predictions for the ground-state binding energies of the $A = 210$–212 Pb and Bi isotopes are in good agreement with experiment as discussed previously.[30] The predicted spectrum is seen to be in fair agreement with experiment. Note that fourteen levels are predicted for $E_x < 700$ keV but only nine are known; in particular, the yrast $J^\pi = 4^-$ through 8^- levels have not been located. A feature of interest not shown in Fig. 11 is the energy spectrum of even-parity states. These follow closely to the even-parity spectrum of ^{210}Bi,[30] with the low-lying 3_1^+ state at 866 keV and the 10_1^+ and 12_1^+ states at 1293 and 1294 keV arising predominantly from $\tilde{\nu}0j_{15/2} \otimes \pi 0h_{9/2}$, where $\tilde{\nu}$ denotes the odd neutron with the other two coupled to 0^+. The lowest 1^+ state appears at 1358 keV and is mainly $\tilde{\nu}0i_{11/2} \otimes \pi 0i_{13/2}$.

In addition to energy spectra, the observables calculated were ^{210}Pb$(\beta^-)^{210}$Bi and ^{212}Pb$(\beta^-)^{212}$Bi decay rates and a few $M1$ transition strengths. For both the β and γ observables, a given matrix element is formulated as

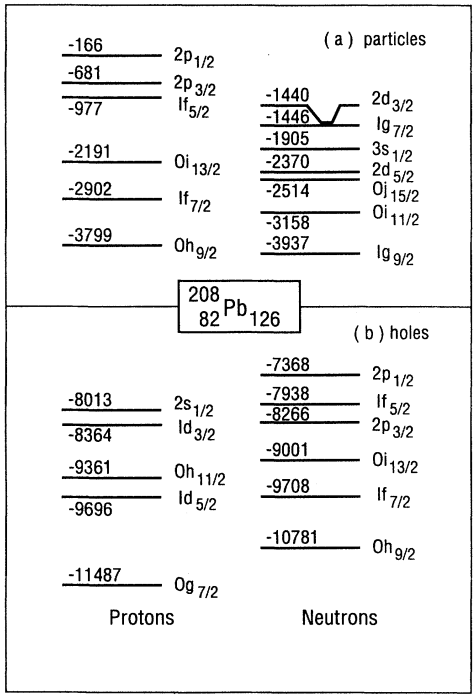

FIG. 10. The Kuo-Herling (KH) model spaces. Single-particle energies are taken from experiment and given in keV.

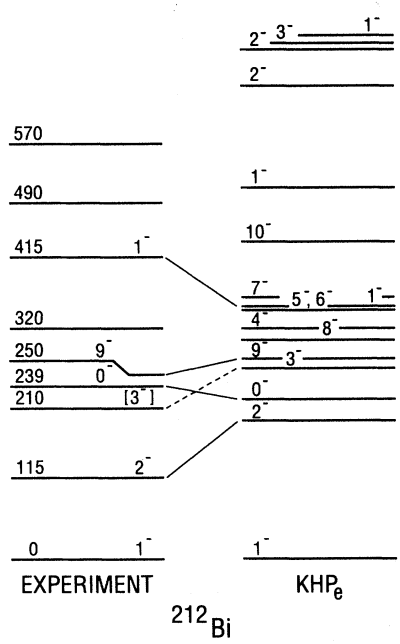

FIG. 11. Comparison to experiment (Ref. 34) of the KHP$_e$ predictions for the low-lying levels of ^{212}Bi.

$$M_R^\alpha = \sum_{j_i j_f} \mathcal{M}_R^\alpha(j_i j_f) = \sum_{j_i j_f} D_R(j_i j_f) q_\alpha(j_i j_f) M_R^\alpha(j_i j_f), \quad (4)$$

where α defines the matrix element of rank R, $M_R^\alpha(j_i j_f)$ is a single-particle matrix element for the transition $j_i \rightarrow j_f$ in the impulse approximation, and the quenching factor $q_\alpha(j_i j_f)$ corrects $M_R^\alpha(j_i j_f)$ for the finite size of the model space and some effects of the nuclear medium. The $D_R(j_i j_f)$ are the one-body transition densities which are the result of the shell-model calculation.

For $M1$ transitions, the $q_{M1}(j_i j_f) M_1^{M1}(j_i j_f)$ are calculated from the effective operators derived by Arima *et al.*[35] from fundamental considerations. For first-forbidden beta decay the matrix elements $M_R^\alpha(j_i j_f)$ are calculated using Woods-Saxon radial wave functions and the $q_\alpha(j_i j_f)$ are evaluated from a consideration of core polarization.[36] For the rank-zero contribution to first-forbidden β decay the selection rule $j_i = j_f$ prevails and there are two matrix elements corresponding to the time-like component of the weak axial-vector current, $M_0^T(j)$, and the space-like component, $M_0^S(j)$. Finally, an appraisal of the overall validity of the core-polarization effects and an evaluation of the non-nucleonic enhancement of M_0^T (see Sec. I) was achieved by a least-squares fit to decays in the $A = 205$–212 region with the overall strength of the rank-one contribution and the non-nucleonic enhancement factor as variables.[1,2] It was found that the normalization factor for rank-one decays was consistent with unity while the non-nucleonic enhancement factor was 2.0. Thus, the effective $q_\alpha(j_i j_f)$ are those of Ref. 36 for the rank-one operators and for $M_0^S(j)$, while for $M_0^T(j)$ it is $2.0 q_\alpha(j_i j_f)$.

B. A generalized seniority model for A =210, 212, and 214 Pb and Bi

The even lead isotopes provide a classic environment for the generalized seniority scheme.[37] Accordingly, the wave functions of the ^{212}Pb(0_1^+) and ^{212}Bi(0_1^-) states were examined to see how well they were approximated by

$$\mathcal{A}\{[^{210}\mathrm{Pb}(0_1^+)] \otimes [^{210}\mathrm{Pb}(0_1^+)]\}_{0+} \quad (5a)$$

and

$$\mathcal{A}\{[^{210}\mathrm{Pb}(0_1^+)] \otimes [^{210}\mathrm{Bi}(0_1^-)]\}_{0-}. \quad (5b)$$

Indeed it was found that Eq. (5a) is a very good approximation to the relationship between the KHP$_e$ wave functions of ^{210}Pb(0_1^+) and ^{212}Pb(0_1^+). There are several ways to demonstrate the applicability of Eq. (5a). One simple way is to compare mean occupation numbers for the seven j orbits in the neutron-particle space of Fig. 10. If we denote the mean occupation of the jth orbit as $\bar{n}(j)$ and the mean partition of the orbits as

$$\bar{\mathcal{P}}[\bar{n}(i_{11/2}), \bar{n}(g_{9/2}), \bar{n}(j_{15/2}), \bar{n}(d_{5/2}), \bar{n}(d_{3/2}), \bar{n}(s_{1/2}), \bar{n}(g_{7/2})], \quad (6)$$

then the model of Eq. (5a) gives $\frac{1}{2}\bar{\mathcal{P}}\{^{212}\mathrm{Pb}(0_1^+)\} = \bar{\mathcal{P}}\{^{210}\mathrm{Pb}(0_1^+)\}$ — where $\frac{1}{2}\bar{\mathcal{P}}$ is symbolic for $\bar{\mathcal{P}}[\frac{1}{2}\bar{n}(i_{11/2})$, etc.]— while the KHP$_e$ calculation gives

$$\bar{\mathcal{P}}\{^{210}\mathrm{Pb}(0_1^+)\} = \bar{\mathcal{P}}[0.361, 1.332, 0.060, 0.035, 0.013, 0.006, 0.192] \quad (7a)$$

and

$$\tfrac{1}{2}\bar{\mathcal{P}}\{^{212}\mathrm{Pb}(0_1^+)\} = \bar{\mathcal{P}}[0.368, 1.325, 0.062, 0.037, 0.013, 0.006, 0.188], \quad (7b)$$

in very good agreement with the seniority model. Because calculations for $A = 214$ Pb and Bi are beyond our resources, comparison of all three $A = 210$, 212, and 214 isotopes of Pb is not possible in the KHP$_e$ model space. However, recent results of Hartree-Fock calculations for these isotopes give mean occupation numbers for ^{210}Pb, ^{212}Pb, and ^{214}Pb in excellent agreement with the seniority scheme.[38]

In the generalized seniority model the low-lying odd-parity spectra of the A =210, 212, and 214 Bi isotopes would be expected to be identical. The experimentally known ^{214}Bi spectrum is compared to the KHP$_e$ spectra of ^{210}Bi and ^{212}Bi in Fig. 12. Recall that the predictions for ^{210}Bi are identical to the experimental spectrum. For ^{212}Bi we choose to display the predicted spectrum rather than the experimental one because it is desirable to have a complete spectrum for this comparison. It is clear that the three spectra are not identical. Departures of the yrast wave functions from generalized seniority in ^{212,214}Bi will be caused by mixing of the wave functions with higher-lying states which have components due to participation of the additional neutron pairs. Such mixing will depress the states. From this point of view we deduce that the 0_1^- states are affected least by such mixing and the mixing increases as J increases from 0 to 3. This is in qualitative agreement with an examination of the wave functions of the ^{210}Bi and ^{212}Bi states. We expect generalized seniority to be a good approximation for the 0_1^- states, to have lesser validity for the $J^\pi = 1^-$, 2^-, and 3^- yrast states, and to be even less applicable

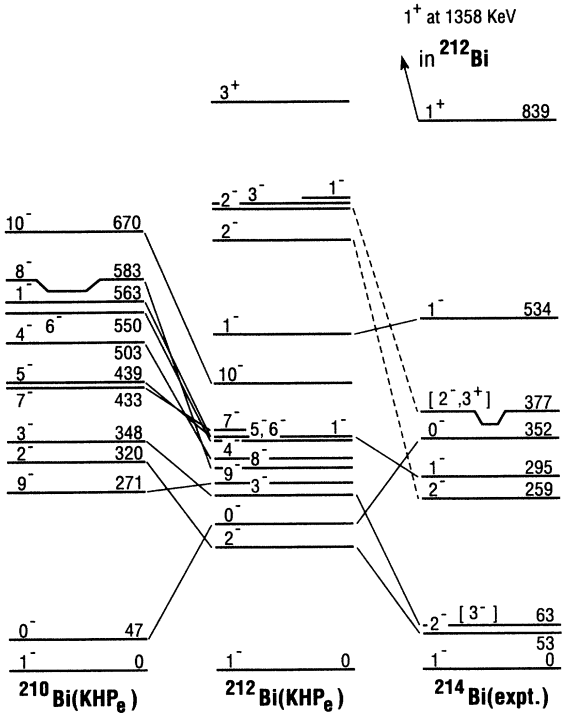

FIG. 12. Comparison of the experimental energy levels of ^{214}Bi to the KHP$_e$ predictions for the spectra of ^{210,212}Bi. The KHP$_e$ prediction for the low-lying spectrum of ^{210}Bi is identical to the experimental one. The predicted and experimental spectra of ^{212}Bi are compared in Fig. 11. The data for ^{214}Bi are from Ref. 6.

(or not applicable at all) for non-yrast states.

For the model of Eq. (5) and its extension to $A = 214$, we have the simple prediction that the $D_R(j)$ of Eq. (4) for $A = 210$, 212, 214 be in the ratio $1, \sqrt{2}, \sqrt{3}$ for all j. Thus a test of Eq. (5) for the ^{212}Bi(0_1^-) state is to compare the $D_R(j)$ for the ^{210}Pb and ^{212}Pb decays. We do this for the 0_1^- states of ^{210}Bi and ^{212}Bi in Table VI. It is clear that the prediction is very well satisfied for the KHP$_e$ model states.

A simple prediction of generalized seniority is that the binding energies of the $A > 208$ even lead isotopes have a linear dependence on A. Only the $A = 210$, 212, 214 masses are known.[39] We display the relationship between them via the two-neutron separation energies (in keV) which are 9122(−160)8962(−202)8760 where the numbers in parentheses are the differences between the adjacent $S(2n)$ which the model predicts to be equal. Since these differences are closely similar (compared to the general situation), the model of Eq. (5a) passes this test quite well. The similar $S(np)$ for the $J^\pi = 0_1^-$ states of ^{210}Bi, ^{212}Bi, and ^{214}Bi are 8393(348)8751(257)9008. Again, the relationship is in good agreement with the model. In conclusion, we feel that the $D_R(j)$ listed in Table VI for β^- decay to the 0_1^- states of both ^{212}Bi and ^{214}Bi are probably a good approximation to the KHP$_e$ interaction and to experiment.

For $q_S(j)M_0^S(j)$ and $q_T(j)M_0^T(j)$ independent of A, Eq. (5) predicts decay rates for ^{212}Bi(0_1^-) and ^{214}Bi(0_1^-) two and three times, respectively, faster than that for ^{210}Bi(0_1^-), with $\log f_0 t$ values correspondingly 0.30 and 0.48 less. However, the $q_S(j)M_0^S(j)$ and $q_T(j)M_0^T(j)$ are not exactly equal for the three decays. The $M_0^S(j)$ and $M_0^T(j)$, as calculated with Woods-Saxon wave functions, differ slightly, e.g., via the nucleon separation energies of the initial and final states, while $q_S(j)$ and $q_T(j)$ depend somewhat on A via the occupation of the $\nu g_{9/2}$ orbit in the initial state.[36] The $D_0(j)q_S(j)M_0^S(j)$ and $D_0(j)q_T(j)M_0^T(j)$ calculated for ^{214}Bi(0_1^-) are listed in Table VI. Also included are results for $j = \frac{11}{2}$ from a proton 1p-1h excitation of the initial state. This result was obtained for ^{210}Pb(β^-)^{210}Bi(0_1^-) in a calculation[1,2] using an interaction operating in a model space (PKH) which consists of the four proton and four neutron orbits just below ^{208}Pb and the three orbits for each just above ^{208}Pb (see Fig. 10). For ^{212}Pb(β^-)^{212}Bi(0_1^-) a similar, but highly truncated, calculation gave a result for the $D_0(11/2)$ essentially equal to that for $A = 210$. It

TABLE VI. The rank-0 $D_0(j)$ for ^{210,212}Pb(0^+)→ ^{210,212}Bi(0^-) and the $M_0^S(j)$ and $M_0^T(j)$ of Eq. (4) for ^{214}Pb(0^+) → ^{214}Bi(0^-).

Orbit		$D_0(j)$	$\sqrt{2}D_0(j)$	$D_0(j)$	$\mathcal{M}_0^S(j)$[a]	$\mathcal{M}_0^T(j)$[a]
ν	π	$A = 210$	$A = 210$	$A = 212$	$A = 214$	$A = 214$
$g_{9/2}$	$h_{9/2}$	0.3612	0.5108	0.4906	−6.0539	84.785
$g_{7/2}$	$f_{7/2}$	−0.0089	−0.0126	−0.0123	−0.247	4.958
$d_{5/2}$	$f_{5/2}$	0.0064	0.0091	0.0093	−0.123	1.485
$d_{3/2}$	$p_{3/2}$	−0.0025	−0.0036	−0.0033	−0.053	0.769
$s_{1/2}$	$p_{1/2}$	0.0019	0.0027	0.0026	−0.023	0.309
$i_{11/2}$	$h_{11/2}$	0.0253		0.0230[b]	0.556	−10.830
				Total	−5.943	81.477

[a]Calculated from Eq. (4) with the $D_0(j)$ taken as $\sqrt{3}$ times the $D_0(j)$ for $A = 210$ listed in the third column.

[b]$D_0(11/2)$ was calculated in a full 1p-1h model space for $A = 210$ and in a truncated 1p-1h model space for $A = 212$. The $A = 214$ value was assumed equal to that for $A = 210$.

should be noted that the contributions of the $\mathcal{M}_0^{S,T}(j)$ to the $M_0^{S,T}$ are coherent with only the $j = \frac{11}{2}$ particle-hole contribution out of phase. Thus, the calculation of the matrix elements is insensitive to reasonable changes in the interaction.

The relationship between f_0t and the M_0^S and M_0^T has been given previously.[40,1,2] The final results for the $\log f_0t$ values of the three $0^+ \rightarrow 0^-$ β^- decays are compared to experiment in Table VII. It is seen that the agreement is good. Also included in the table is a similar comparison for the rank-one decays to the first two 1^- states in ^{212,214}Bi and, since it is the only 1^- state energetically accessible, the ground state of ^{210}Bi. These decays show the same trend of decreasing $\log f_0t$ with increasing A as the rank-zero decays; however, for these rank-one decays we only expect qualitative agreement with the generalized seniority model for two reasons. First, as has been discussed, the model is not expected to work as well for the 1_1^- state and is expected to be even less accurate for the 1_2^- state. Second, for the 1_1^- state the decay is dominated by $\nu g_{9/2} \rightarrow \pi h_{9/2}$ and for this transition the contributions from the three rank-one matrix elements add destructively and almost exactly cancel for $A = 210$. Thus the agreement achieved with the KHP$_e$ model for the ^{210,212}Pb decays to the 1_1^- state is extraordinarily good. The decays to the 1_2^- states in ^{212,214}Bi are a combination of $\nu i_{11/2} \rightarrow \pi h_{9/2}$ and $\nu g_{9/2} \rightarrow \pi f_{7/2}$. The rates are quite fast but sensitive to the relative contributions of the various orbits which are themselves sensitive to the mixing between the 1_2^- and 1_3^- states. In view of this, the predictions are considered to be in satisfactory agreement with experiment.

C. The $0_1^- \rightarrow 1_1^-$ and $2_1^- \rightarrow 1_1^-$ $M1$ transitions in ^{210,212,214}Bi

In the generalized seniority approximation of Eq. (5) electromagnetic transitions in ^{210,212,214}Bi will be equal. From an examination of the KHP$_e$ wave functions for ^{210}Bi and ^{212}Bi we expect this to be a fairly good approximation for the $0_1^- \rightarrow 1_1^-$ and $2_1^- \rightarrow 1_1^-$ $M1$ transitions in ^{210,212,214}Bi. This expectation follows from the approximate validity of the generalized seniority model for the $0^-, 1^-$, and 2^- yrast states of ^{212}Bi and also from the fact that the $0_1^- \rightarrow 1_1^-$ and $2_1^- \rightarrow 1_1^-$ $M1$ transitions in ^{210,212}Bi are very strong and thus relatively insensitive to changes in the wave functions. In both ^{210}Bi and ^{212}Bi the $0_1^- \rightarrow 1_1^-$ and $2_1^- \rightarrow 1_1^-$ $M1$ transitions are rather pure $\pi h_{9/2}\nu g_{9/2} \rightarrow \pi h_{9/2}\nu g_{9/2}$ transitions for which the proton and neutron contributions are constructive. The predictions for the $B(M1)$ values are given in Table VIII along with the data needed to convert them to mean lives, and the predicted and experimental mean lives. The similarity to pure $\pi h_{9/2}\nu g_{9/2} \rightarrow \pi h_{9/2}\nu g_{9/2}$ transitions is exemplified by comparing the ^{210}Bi $0_1^- \rightarrow 1_1^-$ result of $B(M1) = 8.62\mu_N^2$ for the pure configuration to the KHP$_e$ value of $8.59\mu_N^2$. It is also interesting to compare the result for this transition to that corresponding to the use of free-nucleon operators which is $B(M1) = 6.43\mu_N^2$ for the KHP$_e$ interaction. As can be seen in Table VIII, there is a small reduction in the $B(M1)$ values in going from ^{210}Bi to ^{212}Bi as would be expected for a small departure from generalized seniority. We arbitrarily assume the same fractional reduction in going from ^{212}Bi to ^{214}Bi.

The predicted mean lives of Table VIII are seen to be consistent with the rather uninformative experimental information in five of the six cases. The experimental value for the ^{212}Bi $2_1^- \rightarrow 1_1^-$ transition is in disagreement by 1.5 standard deviations — not enough to be of concern in view of the notorious opportunities for systematic error in the centroid shift method[45] by which this experimental value was obtained. A mean life of 7.5 ± 1.5 ps for the 319-keV ^{210}Bi $2_1^- \rightarrow 1_1^-$ transition was measured by Donahue *et al.*[43] using the recoil-distance technique.[45] However, Donahue *et al.* pointed out that this mean life is to be associated with the 319-keV level *and* any unobserved cascades into it. The ^{210}Bi 3_1^- level lies at 347.9 keV, 28.2 keV above the 2_1^- level, so that a 348 → 319 cascade so qualifies; hence the limit shown for the experimental mean life of the ^{210}Bi 2_1^- level in Table VIII. Using the KHP$_e$ interaction and an additional effective charge for both neutrons and protons of $1.0e$, we obtain predicted transition strengths for the ^{210}Bi $3_1^- \rightarrow 1_1^-$ and $3_1^- \rightarrow 2_1^-$ transitions of $B(E2) = 360\ e^2\text{fm}^4$ and $B(M1) = 3.33\mu_N^2$, respectively. When combined with the internal conversion coefficients for pure $E2$ and $M1$ radiation, respectively, these strengths give a $3_1^- \rightarrow 2_1^-$ branching ratio of 98.0%, with 2.0% going to the 1_1^- ground state. This prediction is in good accord with a $3_1^- \rightarrow 2_1^-$ branching ratio of 98.5 ± 0.5 % deduced from the recent (n,γ) results of Sheline *et al.*[46] using the same assumption of pure $E2$ and $M1$ radiation. The KHP$_e$ prediction for the mean

TABLE VII. Comparison of model and experiment for the $\log f_0t$ values of the ^{210,212,214}Pb$(0^+) \rightarrow {}^{210,212,214}Bi(0_1^-, 1_1^-, 1_2^-)$ transitions.

A	$0_1^+ \rightarrow 0_1^-$		$0_1^+ \rightarrow 1_1^-$		$0_1^+ \rightarrow 1_2^-$	
	Expt.	Model	Expt.	Model	Expt.	Model
210	5.468(43)	5.567	7.827(66)	7.838		
212	5.190(20)	5.234	6.809(90)	7.130	5.363(38)	5.632
214	5.088(29)	5.008	6.459(56)	6.954[a]	5.263(27)	5.456[a]

[a]Taken as the predicted $\log f_0t$ for $A = 212$ minus 0.176.

TABLE VIII. KHP$_e$ predictions for $0_1^- \rightarrow 1_1^-$ and $2_1^- \rightarrow 1_1^-$ $M1$ transitions in ^{210,212,214}Bi. The $E2$ contribution to the mean life of the $2_1^- \rightarrow 1_1^-$ transitions is predicted to be negligible. To obtain the $B(M1)$ in single-particle units divide by 1.7905.

		$0_1^- \rightarrow 1_1^-$			$2_1^- \rightarrow 1_1^-$		
Quantity		^{210}Bi	^{212}Bi	^{214}Bi	^{210}Bi	^{212}Bi	^{214}Bi
E_γ	(keV)	46.52	238.63	351.92	319.8	115.18	53.23
$\alpha(M1)$		18.73	0.910	0.313	0.406	7.12	12.62
$B(M1)$	(μ_N^2)	8.59	7.64	6.69[a]	2.94	2.28	1.62[a]
τ(KHP$_e$)	(ps)	3.3	0.29	0.15	0.42	2.0	17.2
τ(expt.)	(ps)	<4300[b]	2±3[c]	≤144[d]	≤7.5±1.5[e]	11±6[f]	≤144[g]

[a] Assuming a linear extrapolation from the $A = 210$ and 212 isotopes.
[b] Reference 41.
[c] Reference 42. This value is erroneously given as 1.5 ± 0.3 ps in Ref. 34.
[d] Reference 11.
[e] Reference 43, see text. This value is incorrectly given as 7.5 ± 1.5 ps in Reference 41.
[f] Reference 44.
[g] Present value.

life of the 3_1^- level is 8.6 ps in excellent agreement with the experimental value[43] of 7.5 ± 1.5 ps which should be associated with the 3_1^- level with no effect from the 2_1^- level.

D. The level schemes of ^{210,212,214}Bi and the 1_1^+ state of ^{214}Bi

The comparison in Fig. 12 indicates an increasing compression of the low-lying odd-parity spectra of the ^{210,212,214}Bi isotopes as A increases. This is particularly noticeable for the 2_2^- levels of ^{212,214}Bi and — if our speculated 2^- assignment for the ^{214}Bi 377-keV level is correct — also for the 2_3^- levels (note, however, that we have indicated the possibility of associating the 377-keV level with the 3_1^+ level as well). As noted in Sec. III B, this compression indicates a significant contribution from the neutron pairs added as A increases from 210 to 214. Another noticeable feature of the comparison is that the experimental spectrum of ^{214}Bi, like that of ^{212}Bi, has numerous missing states, e.g., the yrast 4^- through 10^- states.

A sizable compression is also noticeable for the 1_1^+ state which is predicted at 1929 and 1358 keV in ^{210}Bi and ^{212}Bi, respectively, and lies at 839 keV in ^{214}Bi. The ^{210}Bi 1_1^+ level is a pure $\pi 0i_{13/2}\nu 0i_{11/2}$ state in the KHP$_e$ model space. The ^{212}Bi KHP$_e$ level is fairly well represented as

$$\mathcal{A}\{[^{210}\mathrm{Pb}(0_1^+)] \otimes [^{210}\mathrm{Bi}(1_1^+)]\}_{1+}, \quad (8)$$

i.e., by the generalized seniority scheme. No "intruder" state from outside the KHP$_e$ model space is expected to succeed the predominantly $\pi i_{13/2}$ state as the yrast state in ^{214}Bi and so we associate it with the 839-keV level to which ^{214}Pb decays with $\log f_0 t = 4.56$. Assuming a quenching of the Gamow-Teller matrix element by 0.7, the KHP$_e$ predictions for the hypothetical (i.e., they are not energetically allowed) Pb(0_1^+) → Bi(1_1^+) Gamow-Teller $\log f_0 t$ values are 4.01 and 3.92 for A =212 and 214, respectively. The experimental value for A =214 of 4.56 gives a Gamow-Teller matrix element 2.1 times smaller than the KHP$_e$ prediction for A =212. Clearly, this is an indication that the 1_1^+ state of ^{214}Bi deviates considerably from the predictions of the generalized seniority scheme.

V. SUMMARY AND CONCLUSIONS

The work presented in this paper can be separated into three topics: (i) measurements designed to add information on the spectroscopy of ^{214}Bi and ^{214}Pb(β^-)^{214}Bi, (ii) an analysis of the present and previous measurements to arrive at well-separated "experimental" and "most probable" spin-parity assignments, and (iii) shell-model calculations and application of the generalized seniority scheme to A =210, 212, and 214. Let us summarize these three subjects in turn.

Our measurements of internal conversion coefficients are in agreement with previous results and help to set limits on the amount of $E2$ radiation contributing to predominantly $M1$ transitions (Table II). These limits were set after a careful appraisal of the present and all available previous information. The main finding from the angular correlation measurements is that the levels at 53, 259, 295, 534, and 839 keV have $J > 0$ but the 352-keV level is most probably $J = 0$. A $J = 1$ or 2 assignment is made to the 259-keV level. Lifetime lim-

its were obtained for the 53- and 295-keV levels. The limit $T_{1/2} < 100$ ps for the 53-keV limit is in contrast to the value of 520 ± 150 ps found by Penev *et al.*[11] γ-γ coincidence measurements confirmed the existence of the 63- and 377-keV levels found by Mouze *et al.*[9] via similar measurements. Some incidental γ-ray energy and intensity measurements were made. The γ-ray energies and intensities determined in this work and by Mouze *et al.*[9] were combined by a least-squares-fitting procedure to give "best" level energies, β^- branching ratios and $\log f_0 t$ values (Table IV).

We described the analysis of the present and previous spectroscopic information in Sec. III D. We emphasized that of the known levels of ^{214}Bi (Fig. 1), only the 839-keV level has a definitely known parity. However, the levels at 0, 53, 295, and 352 keV have the same parity. This parity and that of the 259- and 534-keV levels could probably be determined via measurements of the internal conversion of the decays of the 839-keV level. This is certainly true if these decays are essentially pure $E1$ as appears most likely. It is also emphasized that only if local systematics — as formalized by the shell model — are invoked can the parities of the low-lying states be determined. From this point of view the parity of all known states below that at 839 keV are almost certainly odd. However, consideration of the KHP$_e$ shell-model predictions for ^{210,212}Bi suggests the possibility of one or more even-parity levels with $E_x < 839$ keV. We also pointed out that at least seven further levels with $J^\pi = 4^-$ through 10^- are expected in this energy range.

The motivation for this study was an interest in extending our understanding of first-forbidden β decay to higher mass number. It is expected that the $A = 205$-214 nuclei, for which very fast first-forbidden β^- transitions are known,[30] all have single-particle structures which can be explained within the model space of Fig. 10. That is, the collectivity that would bring in further active orbits is not expected so close to the doubly magic ^{208}Pb shell closure. Shell-model calculations for the $A = 210$ and 212 Pb and Bi isotopes are described. These were performed with the m-scheme program OXBASH.[31] Calculations with this program are not presently feasible and so we resort to the simplifying assumption of generalized seniority[37] in order to extend our understanding of the β decay systematics to $A = 214$. In this we are successful: the $\log f_0 t$ values of ^{214}Pb decay can be understood by an extrapolation of the results for ^{210,212}Pb decay. Still a shell-model study of ^{214}Pb decay and a more quantitative exploration of the extent to which generalized seniority works in ^{214}Pb and ^{214}Bi would be of interest. A natural approach would be to perform calculations with a computer program which allows seniority truncation (not possible in the m scheme). It is hoped that this can be done in the near future.

ACKNOWLEDGMENTS

We thank J. B. Cumming for providing the ^{226}Ra source. Research was supported by the U. S. Department of Energy under Contract Nos. DE-AC02-76CH00016, DE-FG02-88ER40417, and W-7405-ENG-82. One of us (C.W.) acknowledges support from the Alexander-von-Humboldt Foundation.

*Permanent address: Nuclear Research Center–Negev, P.O. Box 9001, Beer-sheva 84190, Israel.

[1] E. K. Warburton, in *Proceedings of the Seventh International Symposium on Capture Gamma Ray Spectroscopy and Related Topics,* 1990, edited by R. W. Hoff (AIP, New York, 1991).
[2] E. K. Warburton (unpublished).
[3] K. Kubodera, J. Delorme, and M. Rho, Phys. Rev. Lett. **40**, 755 (1978).
[4] P. Guichon, M. Giffon, J. Joseph, R. Laverrière, and C. Samour, Z. Phys. A **285**, 183 (1978); P. Guichon, M. Giffon, and C. Samour, Phys. Lett. **74B**, 15 (1978).
[5] Y. A. Akovali, Nucl. Data Sheets **55**, 665 (1988) ($A = 214$).
[6] K. S. Toth, Nucl. Data Sheets **21**, 437 (1977) ($A = 214$).
[7] M. Mladjenovic and H. Slätis, Ark. Fys. **8**, 65 (1954).
[8] K. O. Nielsen, O. B. Nielsen, and M. A. Waggoner, Nucl. Phys. **2**, 476 (1956).
[9] G. Mouze, O. Diallo, P. Bechlitch, J. F. Comanducci, and C. Ythier, Radiochim. Acta **49**, 13 (1990).
[10] H. Mach, R. L. Gill, and M. Moszynski, Nucl. Instrum. Methods **A280**, 49 (1989); M. Moszynski and H. Mach, *ibid.* **A277**, 407 (1989); H. Mach, F. K. Wohn, M. Moszyński, R. L. Gill, and R. F. Casten, Phys. Rev. C **41**, 1141 (1990).
[11] I. Penev, W. Andrejtscheff, Ch. Protochristow, and Zh. Zhelev, Z. Phys. A **318**, 213 (1984).
[12] H. Hanewinkel, Diplomarbeit, Universität Köln, 1981; S. Albers, A. Clauberg, A. Dewald, C. Wesselborg, and A. Zilges, Verh. Dtsch. Phys. Ges. (VI) **23**, 227 (1988).
[13] A. Wolf, C. Chung, W. G. Walters, R. L. Gill, M. Shmid, H. I. Liou, M. Stelts, R. Chrien, G. Peaslee, and D. S. Brenner, Nucl. Instrum. Methods **206**, 397 (1983).
[14] V. Zobel, J. Eberth, and E. Eube, Nucl. Instrum. Methods **141**, 329 (1977).
[15] The original published results of Ref. 14 are 241.981(8), 295.213(8), and 351.921(8) keV, respectively, and are relative to a ^{198}Au γ-ray energy standard of 411.794(7) keV. The uncertainties do not include the ±7-eV contribution from that in the ^{198}Au standard. The revised scale uses 411.8044(11) keV for the ^{198}Au γ ray (see Ref. 16). The values of Zobel *et al.* (Ref. 14) quoted in the text are corrected for this revision and can be considered as including the uncertainty in the ^{198}Au standard.
[16] R. G. Helmer, P. H. M. van Assche, and C. van der Leun, At. Data Nucl. Data Tables **24**, 39 (1979).
[17] E. K. Warburton and D. E. Alburger, Nucl. Instrum. Methods **A253**, 38 (1986); G. Wang, E. K. Warburton, and D. E. Alburger, *ibid.* **A272**, 791 (1988).
[18] G. L. Borchert, W. Scheck, and O. W. B. Schult, Nucl. Instrum. Methods **124**, 107 (1975).
[19] It should be noted that the uncertainty of 1.4 eV quoted in

the original measurement (Ref. 20) of the 53.226(14)-keV transition was almost certainly a misprint, i.e., an extra zero was added. This misprint was reproduced in the latest compilation (Ref. 6).

[20]D. E. Muller, H. C. Hoyt, D. J. Klein, and J. W. M. DuMond, Phys. Rev. **88**, 775 (1952).

[21]R. G. Helmer, A. J. Caffrey, R. J. Gehrke, and R. C. Greenwood, Nucl. Instrum. Methods **188**, 671 (1981).

[22]HSICC code, National Nuclear Data Center, Brookhaven National Laboratory, Upton, NY 11973.

[23]L. C. Biedenharn and M. E. Rose, Rev. Mod. Phys. **25**, 729 (1953).

[24]A discrepancy exists in the literature for the relative intensity of the 53-keV γ transition. Relative to $I_\gamma(352) = 35.8$, Lingemann *et al.* (Ref. 25) quoted $I_\gamma = 2.2 \pm 0.4$ and this value is adopted in the *Table of Isotopes* (Ref. 26). On the other hand, the Nuclear Data Sheets (Ref. 6) adopts $I_\gamma = 1.11 \pm 0.05$. To resolve this discrepancy, we measured the relative intensities of the 53- and 352-keV γ lines relative to those of 53- and 356-keV from the decay of ^{133}Ba. With $I_\gamma(352) = 35.8$, we obtained $I_\gamma(53) = 1.11 \pm 0.03$ in excellent agreement with the value adopted in Ref. 6.

[25]E. W. A. Lingeman, J. Konijn, P. Polak, and A. H. Wapstra, Nucl. Phys. **A133**, 630 (1969).

[26]*Table of Isotopes*, edited by C. M. Lederer and V. S. Shirley (Wiley, New York, 1978).

[27]S. Raman and N. B. Gove, Phys. Rev. C **7**, 1995 (1973).

[28]One must be careful here to assure that the 2^+ assignments in question are independent of the ^{214}Pb $\rightarrow$ ^{214}Po $\log f_0 t$ values. For the ^{214}Po 2^+ levels at 1378 and 1730 keV with ^{214}Bi $\rightarrow$ ^{214}Po $\log f_1 t$ values of 8.4 and 7.5, respectively, the spin assignments are definite and are from internal conversion measurements and γ-$\gamma(\theta)$ studies (Ref. 6).

[29]In the generalized seniority model discussed in Sec. IV D, γ transition strengths in ^{210}Bi and ^{214}Bi are predicted to be equal. Assuming this model, we calculate a branching ratio for a 3_1^- 63-keV state to a 1_1^- ground state of 0.1% and a mean life for the 3_1^- state of 40 ps.

[30]E. K. Warburton and B. A. Brown, Phys. Rev. C **43**, 602 (1991).

[31]B. A. Brown, A. Etchegoyen, W. D. M. Rae, and N. S. Godwin, OXBASH, 1984 (unpublished).

[32]T. T. S. Kuo and G. H. Herling, U.S. Naval Research Laboratory Report No. 2258, 1971 (unpublished).

[33]There has been no previous report of a diagonalization of these states in the full Kuo-Herling particle space. The spectrum is available upon request to one of the authors (E.K.W.).

[34]M. J. Martin, Nucl. Data Sheets **27**, 637 (1979) ($A = 212$).

[35]A. Arima, K. Shimzu, W. Bentz, and H. Hyuga, Adv. Nucl. Phys. **18**, 1 (1987).

[36]E. K. Warburton, Phys. Rev. C **42**, 2479 (1990).

[37]I. Talmi, in *Interacting Bosons in Nuclear Physics*, edited by F. Iachello (Plenum, New York, 1979), pp. 79-91.

[38]P. Bouche, P. Quentin, P. Quentin, and M. Weiss, private communication.

[39]A. H. Wapstra and G. Audi, Nucl. Phys. **A432**, 1 (1985).

[40]E. K. Warburton, J. A. Becker, B. A. Brown, and D. J. Millener, Ann. Phys. (N.Y.) **187**, 471 (1988).

[41]B. Harmatz, Nucl. Data Sheets **34**, 735 (1981) ($A = 210$).

[42]J. Lindskog, T. Sundström, J. O. Lindström, and P. Sparrman, Ark. Fys. **24**, 161 (1963).

[43]D. J. Donahue, O. Häusser, R. L. Hershberger, R. Lutter, and F. Riess, Phys. Rev. C **12**, 1547 (1975).

[44]K. G. Välivaara and A. Marelius, Phys. Scr. **3**, 111 (1971).

[45]D. B. Fossan and E. K. Warburton, in *Nuclear Spectroscopy and Reactions, Part C*, edited by J. Cerny (Academic, New York, 1974), p. 307.

[46]R. K. Sheline, R. L. Ponting, A. K. Jain, J. Kvasil, B. bu Nianga, and L. Nkwambiaya, Czech. J. Phys. **B39**, 22 (1989).